J. Marine Sci. Appl. (2012) 11: 478-485
DOI: 10.1007/s11804-012-1158-6

An Unstructured Finite Volume Method for Impact Dynamics of a Thin Plate

Weidong Chen and Yanchun Yu*

Department of Space and Architectural Engineering, Harbin Engineering University, Harbin 150001, China

Abstract: The examination of an unstructured finite volume method for structural dynamics is assessed for simulations of systematic impact dynamics. A robust display dual-time stepping method is utilized to obtain time accurate solutions. The study of impact dynamics is a complex problem that should consider strength models and state equations to describe the mechanical behavior of materials. The current method has several features. 1) Discrete equations of unstructured finite volume method naturally follow the conservation law. 2) Display dual-time stepping method is suitable for the analysis of impact dynamic problems of time accurate solutions. 3) The method did not produce grid distortion when large deformation appeared. The method is validated by the problem of impact dynamics of an elastic plate with initial conditions and material properties. The results validate the finite element numerical data.
Keywords: unstructured finite volume method; structural impact dynamics; large deformation; strength models; state equations
Article ID: 1671-9433(2012)04-0478-08

1 Introduction

Computational structural mechanics (CSM) has been dominated by the finite element method (FEM) and computational fluid dynamics (CFD) have been based on finite volume method (FVM) for the past three decades. The two methods solve the integral governing equations by means of weighted residual methods where they differ in the selected weighting functions. However, their dissimilar properties and applications have resulted in numerical software tools for CFD and CSD that are unlike in almost every aspect. The FVM may be considered as a particular case of the FEM with non-Gale kin weighting (Onate, 1994). Nonetheless, the essential difference between FEM and FVM prudence of second order accurate, partial differential equation is modest and for many applications, the two techniques are equivalent (Idelsohn and Onate, 1994).

In recent years, there have been a series of research efforts to develop FVM to a variety of aspects of CSM. For example, the bending deformation of thick and thin plates has been analyzed using FVM by Wheel (1997). The analyses of stress wave propagation in elastic media have been performed employing FVM by Tielin *et al*. (2004).

The prediction stresses and displacements in thermo-elasto-plastic material have been reported by Demirtzic *et al.* (Demirtzic and Martionvic, 1993; Demirtzic *et al.*, 1994; Demirtzic *et al*., 1997). The analysis of dynamic solid mechanics (Slone *et al*., 2003) and the application to FSI by Slone *et al*. (2004) has also been reported. A control volume procedure for solving the elastic stress-strain equations for two dimensional arbitrarily complex geometries has been shown by Fryer *et al*. (1991). The research illustrates the FVM is competitive with the FEM in terms of numerical accuracy and computational efficiency for CSD problems. Wheel (1996) proved the FVM achieves greater accuracy than the FEM for a NAFEMS (National Agency for FE Methods and Standards) still an elliptic membrane benchmark. The solutions of different CSD problems in addition have been performed by Bailey and Cross (1995), Taylor *et al.* (1995) , Hattel and Hansen (1995). A finite volume method for solid mechanics incorporating rotational degrees of freedom has been reported by Wenke and Wheel (2003).

A cell vertex and cell centered forms of FVM for the analysis of transversely loaded plates has been developed by Fallah (2004). The completion of FVM for CSD computations can be ranged into two classifications: the cell-vertex method and the cell-centered method. In the cell-vertex method, the stress and displacement variables are stored at the vertices of the mesh which themselves enclosed by control volumes. In the cell-centered method, the variables are stored at centroid of cells, which are also used as control volumes themselves. Therefore, the cell-vertex method doesn't need more computational effort and memory for a given mesh. And it is better suited to compute stresses, especially when the meshes become highly distortive. This is the reason why the cell-vertex method is used in this work. With the completion of FVM for structural dynamics, the numerical solutions satisfy both local and global conservations. Furthermore, the cell-vertex method applied

Received date: 2012-10-18.
***Corresponding author Email:** yuyanchunno.1@163.com

in this work does not use shape functions for spatial discretizations and it is matrix-free, thus reducing the computational efforts and memory requirements.

An unstructured finite volume method for structural impact dynamics is introduced, and the results have been compared between the FVM and FEM. Structural impact dynamics are very complex problems; it involved nonlinearity and large deformation. Therefore, strength models and state equations should be added to the structural impact dynamic problems. The display dual-time stepping method, which is suitable for the analysis of impact dynamic problem, was applied to the FVM.

2 Finite volume methods for structural impact dynamics

2.1 Governing equation

As we all known, the governing equations for impact dynamic problems are conservation of mass, conservation of momentum and conservation of energy.

1) Conservation of mass

$$\rho = \frac{\rho_0 V_0}{V} = \frac{m}{V}$$

where ρ is the density; m the mass and V the volume. If it is a two-dimensional problem, the volume V is replaced by area S, and

$$\rho = \frac{\rho_0 S_0}{S} = \frac{m}{S}$$

2) Conservation of momentum

In this paper, two-dimensional problem is considered. So the equations are as follows:

$$\begin{aligned} \rho\ddot{x} &= \frac{\partial \sigma_{xx}}{\partial x} + \frac{\partial \sigma_{xy}}{\partial y} \\ \rho\ddot{y} &= \frac{\partial \sigma_{xy}}{\partial x} + \frac{\partial \sigma_{yy}}{\partial y} \end{aligned} \tag{1}$$

where x and y are the coordinate components in x and y directions respectively.

3) Conservation of energy

$$\dot{e} = \frac{1}{\rho}\left(\sigma_{xx}\dot{\varepsilon}_{xx} + \sigma_{yy}\dot{\varepsilon}_{yy} + 2\sigma_{xy}\dot{\varepsilon}_{xy}\right)$$

where $\dot{\varepsilon}_{xx}$、 $\dot{\varepsilon}_{yy}$ and $\dot{\varepsilon}_{xy}$ are the strain rate.

4) Constitutive model

Impact dynamic problems are fairly complex, it involves in material non-linearity, geometrical non-linearity and boundary condition non-linearity. Therefore, it is important to choose appropriate constitutive model to describe the mechanics behavior of materials. Elastoplasticity constitutive model is used in this study.

5) Stress tensor

The stress tensor is separated into a hydrostatic component p and a deviatoric component

$$\sigma_{xx} = -(p+q) + s_{xx}$$

$$\sigma_{yy} = -(p+q) + s_{yy}$$

$$\sigma_{xy} = s_{xy}$$

where q is the pseudo-viscous force. The negative sign for the hydrostatic pressure p follows from the usual notation that stresses are positive in tension and negative in compression.

6) Strain tensor

The strain tensor ε_{ij} is determined from the relation between the strain rates and the velocities $(\dot{x}, \dot{y})$

$$\dot{\varepsilon}_{xx} = \frac{\partial \dot{x}}{\partial x}$$

$$\dot{\varepsilon}_{yy} = \frac{\partial \dot{y}}{\partial y}$$

$$\dot{\varepsilon}_{xy} = \frac{1}{2}\left[\frac{\partial \dot{x}}{\partial y} + \frac{\partial \dot{y}}{\partial x}\right]$$

And these strain rates are related to the rate of change of volume by

$$\frac{\dot{V}}{V} = \dot{\varepsilon}_{xx} + \dot{\varepsilon}_{yy} \tag{2}$$

7) Deviatoric stress rate

For elastic behavior of a material we may derive from equation (2) and Hooke's Law relations between the deviatoric stress rates and the strain rates

$$\dot{s}_{xx} = 2G\left[\dot{\varepsilon}_{xx} - \frac{1}{3}\frac{\dot{V}}{V}\right]$$

$$\dot{s}_{yy} = 2G\left[\dot{\varepsilon}_{yy} - \frac{1}{3}\frac{\dot{V}}{V}\right]$$

$$\dot{s}_{xy} = 2G\dot{\varepsilon}_{xy}$$

8) Equation of state

The pressure p is related to the density ρ and specific internal energy e through an equation of state

$$p = f(\rho, e)$$

2.2 Special discretization

Eq.(1) is discretized on an unstructured triangular grid and a cell-vertex scheme is adopted to construct control volumes (Xia *et al*., 2007). The spatial discretization is performed by using the integral form of the conservation equations over the control volume surrounding node k shown in Fig. 1.

$$\int_S \rho \ddot{x} \mathrm{d}S = \int_S \left(\frac{\partial \sigma_{xx}}{\partial x} + \frac{\partial \sigma_{xy}}{\partial y} \right) \mathrm{d}S$$
$$\int_S \rho \ddot{y} \mathrm{d}S = \int_S \left(\frac{\partial \sigma_{xy}}{\partial x} + \frac{\partial \sigma_{yy}}{\partial y} \right) \mathrm{d}S \tag{3}$$

The right-hand side of the Eq. (3) is converted to a line integral via the divergence theorem of Gauss, and it is given as

$$\int_S \frac{\partial \sigma_{ji}}{\partial x_j} \mathrm{d}S = \oint_l \sigma_{ji} n_i \mathrm{d}l$$

And the Eq. (3) then are approximated by

$$\int_S \rho \ddot{x} \mathrm{d}x\mathrm{d}y = \oint_l \sigma_{xx} \mathrm{d}y - \sigma_{xy} \mathrm{d}x$$
$$\int_S \rho \ddot{y} \mathrm{d}x\mathrm{d}y = \oint_l \sigma_{xy} \mathrm{d}y - \sigma_{yy} \mathrm{d}x \tag{4}$$

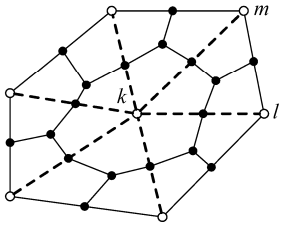

Fig. 1 Construction of the control volume for node *k*.

where l is the control volume boundary. And the right-hand side of the Eq.(4) is approximated by

$$\oint_l \sigma_{xx} \mathrm{d}y - \sigma_{xy} \mathrm{d}x = \sum_{n=1}^{n_{k3}} \int_{l_{kn}} \sigma_{xx} \mathrm{d}y - \sum_{n=1}^{n_{k3}} \int_{l_{kn}} \sigma_{xy} \mathrm{d}x$$
$$\oint_l \sigma_{xy} \mathrm{d}y - \sigma_{yy} \mathrm{d}x = \sum_{n=1}^{n_{k3}} \int_{l_{kn}} \sigma_{xy} \mathrm{d}y - \sum_{n=1}^{n_{k3}} \int_{l_{kn}} \sigma_{yy} \mathrm{d}x \tag{5}$$

where n_{k3} is the total number of triangular cells associated with node k. l_{kn} is the part of control volume boundary in the n triangular cell associated with node k. Based on the constant stresses assumption, the integrals in each triangular cell in Eq. (5) simply reduce to $(\sigma_{xx})_n (a_k)_n - (\sigma_{xy})_n (b_k)_n$ and $(\sigma_{xy})_n (a_k)_n - (\sigma_{yy})_n (b_k)_n$.

For a typical control volume including node k inside the medium, by applying the mass model to the discrete system, the left-hand side of the Eq. (3) $M_k \ddot{u}_{xk}$ and $M_k \ddot{u}_{yk}$ respectively. Here M_k is the mass of the control volume including node k. $\ddot{u}_{xk}$ and $\ddot{u}_{yk}$ are the acceleration components of node k in x and y directions respectively. Finally, the following equations are obtained:

$$M_k \ddot{u}_{xk} = \sum_{n=1}^{n_{k3}} (\sigma_{xx})_n (a_k)_n - \sum_{n=1}^{n_{k3}} (\sigma_{xy})_n (b_k)_n$$
$$M_k \ddot{u}_{xk} = \sum_{n=1}^{n_{k3}} (\sigma_{xx})_n (a_k)_n - \sum_{n=1}^{n_{k3}} (\sigma_{xy})_n (b_k)_n \tag{6}$$

where $(a_k)_n$ and $(b_k)_n$ are respectively the coefficients for the node k of the n th triangular cell around node k. Here $a_k = (y_l - y_m)/2$ $a_l = (y_m - y_k)/2$ $a_m = (y_k - y_l)/2$ $b_k = (x_m - x_l)/2$ $b_l = (x_k - x_m)/2$ $b_m = (x_l - x_k)/2$. And (x_k, y_k), (x_l, y_l) and (x_m, y_m) are coordinates of node k, l and m respectively. $(\sigma_{xx})_n$, $(\sigma_{xy})_n$ and $(\sigma_{yy})_n$ are the stresses of the n triangular cell around node k.

For a typical control volume including node m on the surface of the medium, also by applying the mass model to the discrete system, the left-hand side of the Eq. (4) are $M_m \ddot{u}_{xm}$ and $M_m \ddot{u}_{ym}$ respectively. Here M_m is the mass of the control volume including node m. $\ddot{u}_{xm}$ and $\ddot{u}_{ym}$ are the acceleration components of node m in x and y directions respectively. The right-hand side of the Eq. (4) is

$$\oint_l \sigma_{xx} \mathrm{d}y - \sigma_{xy} \mathrm{d}x = \sum_{n=1}^{n_{m3}} \int_{l_{mn}} \sigma_{xx} \mathrm{d}y - \sum_{n=1}^{n_{m3}} \int_{l_{mn}} \sigma_{xy} \mathrm{d}x + \int_{a \to m \to b} \bar{X} \mathrm{d}l$$

$$\oint_l \sigma_{xy} \mathrm{d}y - \sigma_{yy} \mathrm{d}x = \sum_{n=1}^{n_{m3}} \int_{l_{mn}} \sigma_{xy} \mathrm{d}y - \sum_{n=1}^{n_{m3}} \int_{l_{mn}} \sigma_{yy} \mathrm{d}x + \int_{a \to m \to b} \bar{Y} \mathrm{d}l$$

where l_{mn} is the part of control volume boundary in the n th triangular cell associated with node m. n_{m3} is the total number of triangular cells associated with node m. $\bar{X}$ and $\bar{Y}$ are the densities of external force on the surface in x and y directions respectively.

Finally, the following equations are obtained:

$$M_m \ddot{u}_{xm} = \sum_{n=1}^{n_{m3}} (\sigma_{xx})_n (a_m)_n - \sum_{n=1}^{n_{m3}} (\sigma_{xy})_n (b_m)_n + \int_{a \to m \to b} \bar{X} \mathrm{d}l$$
$$M_m \ddot{u}_{ym} = \sum_{n=1}^{n_{m3}} (\sigma_{xy})_n (a_m)_n - \sum_{n=1}^{n_{m3}} (\sigma_{yy})_n (b_m)_n + \int_{a \to m \to b} \bar{Y} \mathrm{d}l \tag{7}$$

where the coefficients $(a_m)_n$ and $(b_m)_n$ for the surface node m are similar to the coefficients for the node k. $(\sigma_{xx})_n$, $(\sigma_{xy})_n$ and $(\sigma_{yy})_n$ have the same characteristics.

On the left-hand side of Eq.(6) and Eq.(7), the calculation of mass control volume needs to be implemented in within the

method. First, the mass of a triangular cell must be calculated, and then the mass of this cell is assigned to the cell nodes (one-third of the mass for each node of triangular cell). Through circulating all the cells and making a mass assignment as mentioned above, the mass of each control volume for the left-hand side of Eq. (6) can be calculated in the form of

$$M_q = \sum_{n=1}^{n_{q3}} \frac{m_{3qn}}{3}$$

where q can be any node of the elastic medium; for example $q = k$ is the inner node and $q = m$ is the surface node of the medium. m_{3qn} is the mass of the n th triangular cell around node q . n_{q3} is the total number of triangular cells associated with node q .

The stresses σ_{xx} , σ_{xy} and σ_{yy} of all the triangular cells are used at time t . Based on summation of these forces at each node by circulating all the cells, the values of the right-hand side of Eq. (6) for any inner node k have been obtained, thus the quantities $\ddot{u}_{xk}$ and $\ddot{u}_{yk}$ are given at time t . The velocity components of node k at time $t + \Delta t / 2$ can be obtained by using time integration

$$\begin{aligned} \dot{u}_{xk}\left(t + \Delta t/2\right) &= \dot{u}_{xk}\left(t - \Delta t/2\right) + \ddot{u}_{xk}\Delta t \\ \dot{u}_{yk}\left(t + \Delta t/2\right) &= \dot{u}_{yk}\left(t - \Delta t/2\right) + \ddot{u}_{yk}\Delta t \end{aligned} \qquad (8)$$

Initial velocities and accelerations are zeros within a control volume due to the preliminary condition and initial impact load being generally zero at time 0. This tells us that the velocities at times $-\Delta t / 2$ are zero from Taylor's expansion.

Then the displacement components u_{xk} and u_{yk} of node k at time $t + \Delta t$ can be obtained by using time integration

$$\begin{aligned} u_{xk}\left(t + \Delta t\right) &= u_{xk}\left(t\right) + \dot{u}_{xk}\left(t + \Delta t/2\right)\cdot\Delta t \ , \\ u_{yk}\left(t + \Delta t\right) &= u_{yk}\left(t\right) + \dot{u}_{yk}\left(t + \Delta t/2\right)\cdot\Delta t \end{aligned} \qquad (9)$$

The error in Taylor expansions of accelerations $\ddot{u}_{xk}$ and $\ddot{u}_{yk}$ is of order $\left(\Delta t\right)^2$ from Eq. (8), and from Eq. (9), the error in Taylor expansions of velocities $\dot{u}_{xk}$ and $\dot{u}_{yk}$ is also of order $\left(\Delta t\right)^2$. So the accuracy of this method is second-order accurate in time domain discretization. Finally, the stresses σ_{xx} , σ_{xy} and σ_{yy} of all the triangular cells at time $t + \Delta t$ can be obtained according to the constitutive equations. As for any control volume on the surface, the little difference is that external forces exerting on the control volume at time t should be added in the summation of forces for each node on the surface. Therefore, the whole stress field and the whole displacement field are obtained at time $t + \Delta t$. The whole stress field is updated from time t to time $t + \Delta t$, the whole velocity field is updated from time $t - \Delta t / 2$ to time $t + \Delta t / 2$, and the whole displacement field is updated from time t to time $t + \Delta t$.

2.3 Stress update

Cauchy stress tensor can be broken down into deviatoric stress tensor s_{ij} and hydrostatic pressure p :

$$\sigma_{ij} = s_{ij} - p\delta_{ij}$$

The deviatoric stress tensor s_{ij} is updated according to the constitutive model, and the hydrostatic pressure p is by the state equation.

2.3.1 Deviatoric stress update

Elastoplasticity constitutive model is used in this study. Jaumann stress rate σ_{ij}^{∇} is used in constitutive model due to it is free from rotations of rigid bodies.

In the elastic stage, the relationship between deviatoric stress Jaumann rate and deviatoric strain rate is:

$$s_{ij}^{\nabla} = 2G\dot{\varepsilon}_{ij}^{'}$$

where the deviatoric stress Jaumann rate is

$$s_{ij}^{\nabla} = \dot{s}_{ij} - s_{ip}\Omega_{jp} - s_{jp}\Omega_{ip}$$

First, assume that the material is in the elastic stage, the tentative value of the deviatoric stress tensor at time t^{n+1} is:

$${}^{*}s_{ij}^{n+1} = s_{ij}^{n} + \dot{s}_{ij}^{n+1/2}\Delta t^{n+1/2} = s_{ij}^{R^n} + 2G\Delta\varepsilon_{ij}^{'n+1/2}$$

where,

$$\begin{aligned} s_{ij}^{R^n} &= s_{ij}^{n} + s_{ip}^{n}\Omega_{jp}^{n+1/2} + s_{jp}^{n}\Omega_{ip}^{n+1/2} \\ \Delta\varepsilon_{ij}^{'n+1/2} &= \dot{\varepsilon}_{ij}^{'n+1/2}\Delta t^{n+1/2} \end{aligned}$$

The tentative value of effective stress is

$$s^{*n+1} = \left(\frac{3}{2}\,{}^{*}s_{ij}^{n+1}\,{}^{*}s_{ij}^{n+1}\right)^{\frac{1}{2}} \qquad (10)$$

If the tentative value of effective stress s^{*n+1} is greater than the yield stress σ_y^{n+1} , based on Mises yield conditions it is known that

$$F = \frac{3}{2}s_{ij}s_{ij} - \sigma_y^2 \le 0$$

Now it does not meet the Mises yield conditions; tentative stress point ${}^{*}s^{n+1}$ falls on the outside of the yield surface. Scaling down the tentative stress ${}^{*}s^{n+1}$ by the radial return method:

$$s_{ij}^{n+1} = m^* s_{ij}^{n+1} \tag{11}$$

$$m = \frac{\sigma_y^{n+1}}{s^{*n+1}} \tag{12}$$

Plastic strain increment $\Delta\varepsilon_{ij}^p$ is

$$\Delta\varepsilon_{ij}^p = \Delta\varepsilon_{ij}^{'} - \frac{1}{2G}\left(s_{ij}^{n+1} - s_{ij}^{R^n}\right) \tag{13}$$

where

$$\Delta\varepsilon_{ij}^{'} = \frac{^*s_{ij}^{n+1} - s_{ij}^{R^n}}{2G} \tag{14}$$

Substituting Eq. (14) into Eq. (13), then

$$\Delta\varepsilon_{ij}^p = \frac{^*s_{ij}^{n+1} - s_{ij}^{n+1}}{2G} \tag{15}$$

Substituting Eq. (11) into Eq. (15)

$$\Delta\varepsilon_{ij}^p = \left(\frac{1-m}{2G}\right)^* s_{ij}^{n+1} = \lambda s_{ij}^{n+1} \tag{16}$$

where

$$\lambda = \frac{1-m}{2Gm}$$

According to Eq. (10), Eq. (12) and Eq. (16), the effective plastic strain increment is

$$\Delta\varepsilon^p = \left(\frac{2}{3}\Delta\varepsilon_{ij}^p\Delta\varepsilon_{ij}^p\right)^{\frac{1}{2}} = \left[\frac{2}{3}\left(\frac{1-m}{2G}\right)^2\frac{2}{3}s^{*n+1^2}\right]^{\frac{1}{2}} = \frac{s^{*n+1} - \sigma_y^{n+1}}{3G} \tag{17}$$

For the isotropic strengthen problem:

$$\sigma_y^{n+1} = \sigma_y^n + E^p\Delta\varepsilon^p \tag{18}$$

where E^p is plastic hardening modulus.

$$E^p = \frac{EE_t}{E - E_t}$$

where E_t $(= d\sigma / d\varepsilon)$ is tangent modulus, E is modulus of elasticity.

Substituting Eq. (18) into Eq. (17), the following equation is obtained:

$$\Delta\varepsilon^p = \frac{s^{*n+1} - \sigma_y^n - E^p\Delta\varepsilon^p}{3G}$$

Then,

$$\Delta\varepsilon^p = \frac{s^{*n+1} - \sigma_y^n}{3G + E^p}$$

In conclusion, the deviatoric stress updating algorithm can be described as follows:

If the tentative value of effective stress s^{*n+1} is greater than the yield stress σ_y. Then

1) Calculating the plastic strain increment

$$\Delta\varepsilon^p = \frac{s^{*n+1} - \sigma_y^n}{3G + E^p}$$

2) Updating the plastic strain

$$\varepsilon^{pn+1} = \varepsilon^{pn} + \Delta\varepsilon^p$$

3) Updating the yield stress

$$\sigma_y^{n+1} = \sigma_y^n + E^p\Delta\varepsilon^p$$

4) Calculating the scale factor

$$m = \frac{\sigma_y^{n+1}}{s^{*n+1}}$$

5) Making the tentative stress point return to yield surface with the radial return method

$$s_{ij}^{n+1} = m^* s_{ij}^{n+1}$$

$$s^{n+1} = ms^{*n+1}$$

where s^{n+1} is effective stress.

2.3.2 Pressure update

Pressure p is described by state equations

$$p = p(V, E) = p(V, T)$$

Pressure is a function of volume and internal energy; we need to find the integral of the energies equation before calculating the pressure p at times t^{n+1}, the inner energy of every element at time t^{n+1} are

$$e^{n+1} = e^n + V^{n+1/2}s_{ij}^{n+1/2}\Delta\varepsilon_{ij}^{n+1/2} - V^{n+1/2}\left(p^{n+1/2} + q^{n+1/2}\right)\Delta\varepsilon_{kk}^{n+1/2} \tag{19}$$

where,

$$V^{n+1/2} = \frac{1}{2}\left(V^n + V^{n+1}\right)$$

$$s_{ij}^{n+1/2} = \frac{1}{2}\left(s_{ij}^n + s_{ij}^{n+1}\right)$$

Due to $V^{n+1/2}\Delta\varepsilon_{kk}^{n+1/2} = V^{n+1} - V^n = \Delta V$ and $p^{n+1/2} = \left(p^n + p^{n+1}\right)/2$, the Eq. (19) can be considered as

$$e^{n+1} = e^{*n+1} - \frac{1}{2}\Delta V p^{n+1} \tag{20}$$

where

$$e^{*n+1} = e^n - \frac{1}{2}\Delta V p^n - \Delta V q^{n+1/2} + V^{n+1/2} s_{ij}^{n+1/2} \Delta\varepsilon_{ij}^{n+1/2}$$

e^{*n+1} is the estimate of element internal energy at time t^{n+1}.

The common form of state equations can be obtained as follows:

$$p^{n+1} = A\left(V^{n+1}\right) + B\left(V^{n+1}\right)E^{n+1} \tag{21}$$

Where

$$E^{n+1} = \frac{e^{n+1}}{V_0} \tag{22}$$

Substituting Eq. (22) and Eq. (20) into Eq. (21), the pressure p at time t^{n+1} is obtained as follows:

$$p^{n+1} = \frac{A^{n+1}\left(V^{n+1}\right) + B^{n+1}\left(V^{n+1}\right)E^{*n+1}}{1 + \frac{1}{2}B^{n+1}\left(V^{n+1}\right)\frac{\Delta V}{V_0}}$$

$E^{*n+1} = e^{*n+1} / V_0$.

2.3.3 Calculation procedure of the FVM for structural impact dynamics

The flow chart of solving the impact dynamics by the FVM is given in Fig.2.

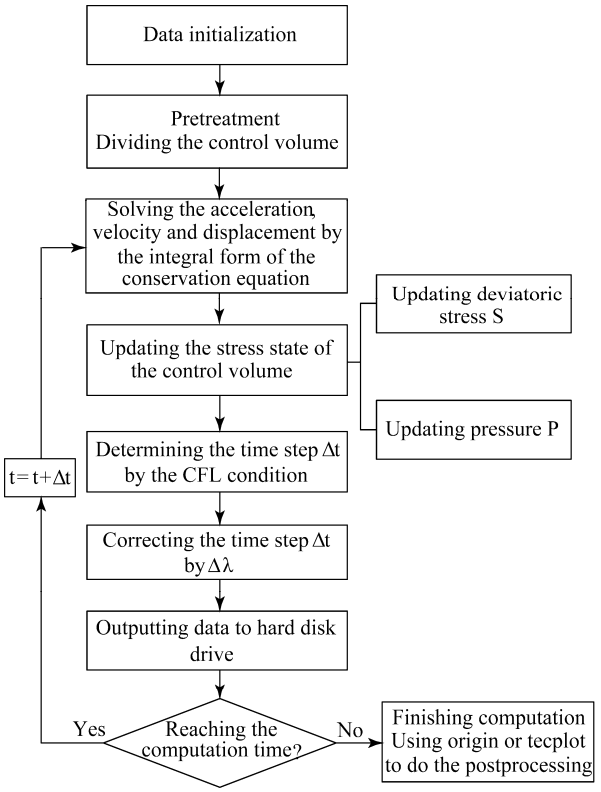

Fig. 2 Flow chart of the FVM

3 Stability analyses

We study the stability analysis according to discussion of the dispersion relations of the displacement finite-difference equations for the infinite medium as the reference (Tielin et al., 2004). For simplicity, the equilateral triangle grids are used in the method.

For the equilateral triangle grids, the finite-difference equations of the method have been referenced by (Tielin et al., 2004) within the research paper. Assuming a plane wave with the frequency of an infinite medium, the displacement components at any point can be described as follows:

$$\left\{u_x \quad u_y\right\}^{\mathrm{T}} = \left\{u_{x0} \quad u_{y0}\right\}^{\mathrm{T}} \exp\left[\mathrm{i}\left(\boldsymbol{k}\cdot\boldsymbol{r} - \omega t\right)\right] \tag{23}$$

Where $\vec{k}$ is the vector of wave number, $\boldsymbol{r}$ is the radius vector, and $\left\{u_{x0} \quad u_{y0}\right\}^{\mathrm{T}}$ is the displacement vector at the origin of the coordinate system at initial time. Substituting Eq. (23) into the finite-difference equations given in the reference (Tielin *et al*., 2004), finally we can obtain the dispersion relations for the equilateral triangle grids method as follows:

$$\sin^2\left(\omega\Delta t/2\right) = \frac{\Delta t^2}{12\Delta x^2}\left\{\left(c_p^2 + c_s^2\right)\left[6 - 4\cos\left(\frac{\Delta x}{2}k_x\right)\cos\left(\frac{\sqrt{3}}{2}\Delta x k_y\right) - 2\cos\left(\Delta x k_x\right) \pm 4\left(c_p^2 - c_s^2\right)\times \sqrt{\left[\cos\left(\frac{\Delta x}{2}k_x\right)\cos\left(\frac{\sqrt{3}}{2}\Delta x k_y\right) - \cos\left(\Delta x k_x\right)\right]^2 + 3\left[\sin\left(\frac{\Delta x}{2}k_x\right)\sin\left(\frac{\sqrt{3}}{2}\Delta x k_y\right)\right]^2}\right\}$$

It is required that $0 \le \sin^2\left(\omega\Delta t/2\right) \le 1.0$ for stability. Finally it can be approximately obtained:

$$\Delta t \le \Delta x / \sqrt{2c_p^2}$$

4 Numerical examples

The calculation model is shown in Fig. 3. This is a plane strain problem. There is a thin plate whose right side and left side are fixed. The shock wave which spreads from a distance works on the slim plate. The side of the thin plate is 1.0 m×0.02 m (the length of the slender plate is 1.0 m, the thickness of the thin plate is 0.02 m). The thin plate is meshed 500×10, and the elements are triangle mesh. Elastoplasticity constitutive model is used in this example. The zoom coefficient of the time step is considered as 0.8. The material parameters are given in Tab.1 which comes from the material database of LS—DYNA software.

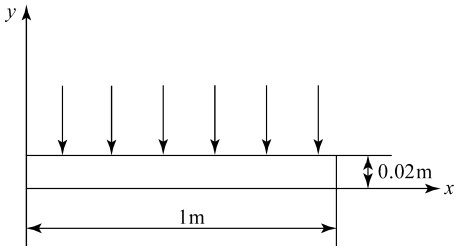

Fig. 3 The calculation model

Table 1 Material parameters

Material	Density /(kg·m^{-3})	Modulus of elasticity /Pa	Tangent modulus /Pa	Yield stress /Pa	Poisson's ratio /Pa
Steel	7830	2.07×10^{11}	5.0×10^{9}	4.0×10^{9}	0.3

Enhanced results can also be obtained by FEM in this example. The accuracy of the calculation has been approved. Therefore it is feasible to validate the accuracy of the FVM according to the FEM.

For comparison, the computation modules for FEM and FVM are the same, the shapes and the sizes of the grids are consistent. The results are given in the Fig. 4 to Fig. 9

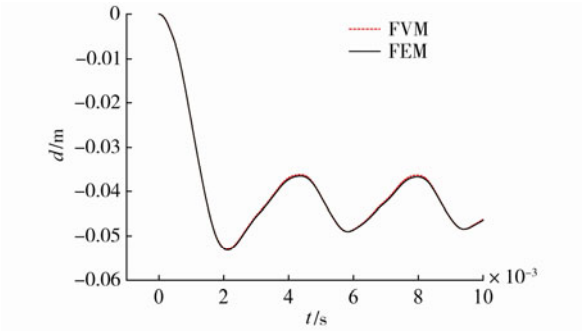

Fig. 4 the displacement curve at point (0.5m，0.02m)

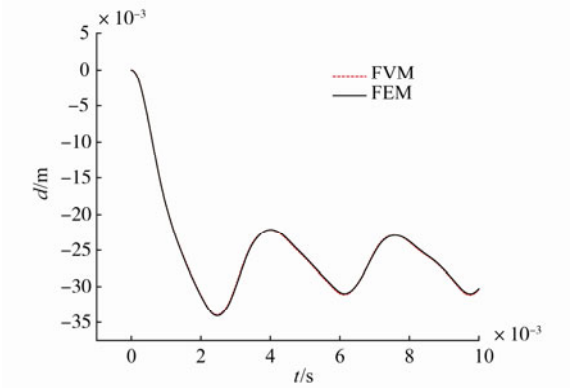

Fig. 5 the displacement curve at point (0.75m，0.02m)

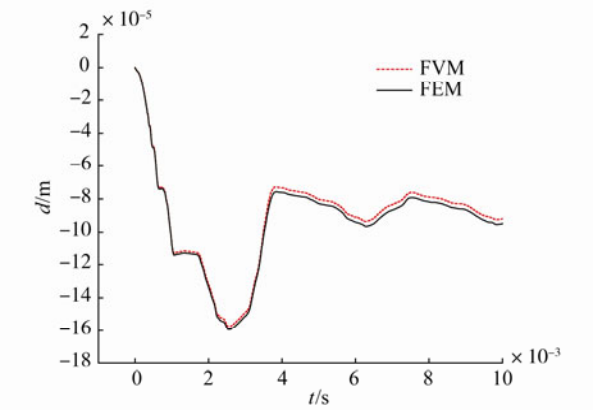

Fig. 6 the displacement curve at point (0.998m，0.02m)

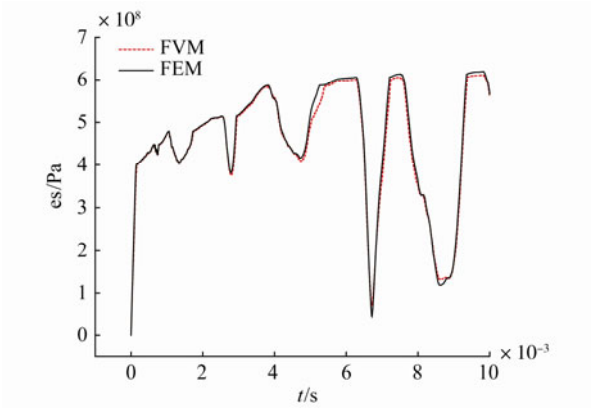

Fig. 7 the stress curve at point (1m，0.019m)

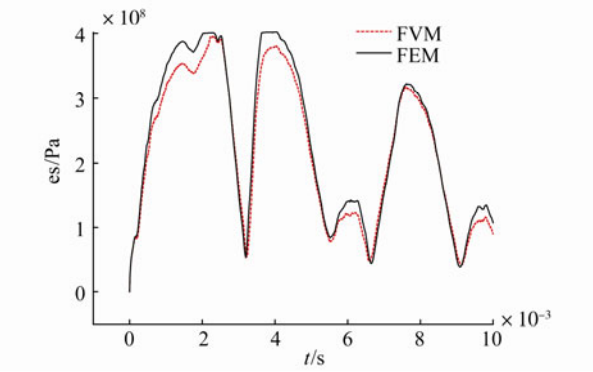

Fig. 8 the stress curve at point (1m，0.01m)

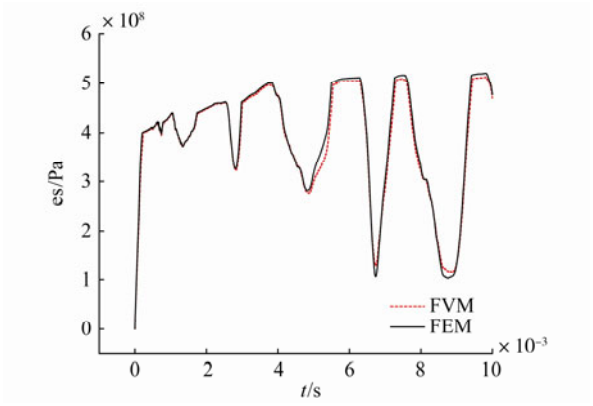

Fig. 9 the stress curve at point (1m，0.01m)

According to the results in Fig.4 to Fig.9, the relationships between deformation and time, and the relationships between effective stress and time in FVM are approved in FEM. The accuracy for the two methods is mainly the same. Therefore, it is feasible to solve the impact dynamic problems with the FVM. In addition, the discrete processes of the FVM are relatively simple and are easy to understand. The physical meaning of the discrete equations is explicit, and the conservation of the discrete equations can be obtained. By using display dual-time stepping method, the present method is more efficient than the traditional FEM, since its greatest strength is not necessary to setup a stiffness matrix and to solve the large system of linear equations, it does not tend to produce grid distortion when large deformation appeared.

5 Conclusions

An unstructured finite volume method is put forward to simulate structural impact dynamics, which consider the large deformation. Structural impact dynamics is a very complex problem; it involves nonlinearity and large deformation issues. Therefore, strength models and state equations need to be added to the structural impact dynamic problems. The case of the thin plate is used to validate the correctness and feasibility of the proposed new method. The computation results of the thin plate case are in good accord with those of the FEM based on commercial software LS-DYNA.

The current methods can be applied for solving the large deformation impact dynamics for thin plate structures. By means of utilizing a display dual-time stepping method, the FVM is more efficient than the traditional FEM, which is expensive in setting up a stiffness matrix and solving the large system of linear equations. Other large deformation problems of complex structures can be researched utilizing the new method.

References

Bailey C, Cross M (1995). A finite volume procedure to solve elastic solid mechanics problems in three dimensions on an unstructured mesh. *International Journal for Numerical Methods in Engineering*, **38**, 1756-1776.

Demirdzic I, Martinovic D (1993). Finite volume method for thermo-elasto-plastic stress analysis. *Computational Methods Applied in Mechanical Engineering*, **109**, 331-349

Demirdzic I, Muzaferija S, Peric M (1994). Finite volume method for stress analysis in complex domains. *International Journal for Numerical Methods in Engineering*, **37**, 3751-3766.

Demirdzic I, Muzaferija S, Peric M (1997). Benchmark solutions of some structural analysis problems using finite volume method and multi-grid acceleration. *International Journal for Numerical Methods in Engineering*, **40**, 1893-1908.

Fallah N (2004). A cell vertex and cell centered finite volume method for plate bending analysis. *Computational Methods Applied in Mechanical Engineering*, **193**, 3457-3470.

Fryer YD (1991). A control volume procedure for solving the elastic stress-strain equations on an unstructured mesh. *Applied Mathematical Modeling*, **15**, 639-645.

Hattel JH, Hansen PN (1995). A control volume-based finite difference method for solving the equilibrium equations in terms of displacements. *Applied Mathematical Modeling*, **19**, 210-243.

Idelsohn SR, Onate E (1994). Finite volumes and finite elements: "two good friends". *International Journal for Numerical Methods in Engineering*, **37**, 3323-3341.

Onate E, Cervera M, Zienkiewicz OC (1994). A finite volume method format for structural mechanics. *International Journal for Numerical Methods in Engineering*, **37**, 181-201.

Slone AK, Bailey C, Cross M (2003). Dynamic solid mechanics using finite volume methods. *Applied Mathematical Modeling*, **27**, 69–87.

Slone AK (2004). A finite volume unstructured mesh approach to dynamic fluid–structure interaction: an assessment of the challenge of predicting the onset of flutter. *Applied Mathematical Modeling* , **28**, 239-311.

Taylor GA, Bailey C, Cross M (1995). Solution of the elastic/visco-plastic constitutive equations: a finite volume approach. *Applied Mathematical Modeling*, **19**, 746-760.

Tielin Liu, Kaishin Liu, Jinxiang Zhang (2004). Unstructured grid method for stress wave propagation in elastic media. *Computational Methods Applied in Mechanical Engineering* **193**, 2427–2452.

Wheel MA (1996). A geometrically versatile finite volume formulation for plane strain elastostatic stress analysis. *Journal of Strain Analysis for Engineering Design*, **31**, 111-116.

Wheel MA (1997). A finite volume method for analyzing the bending deformation of thick and thin plates. *Computational Methods Applied in Mechanical Engineering*, **147**, 199-208.

Wenke P, Wheel MA (2003). A finite volume method for solid mechanics incorporating rotational degrees of freedom. *Computers and Structures*, **81**, 321-329.

Xia GH (2007). A 3D implicit unstructured-grid finite volume method for structural dynamics. *Computational Methods Applied in Mechanical Engineering*, **40**, 299-312.

Weidong Chen was born in 1966. He is a professor and doctoral supervisor at Harbin Engineering University. His research interests are structural reliability, optimal design and explosion mechanics.

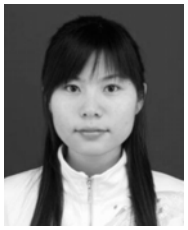

Yanchun Yu was born in 1984. She is a doctoral candidate at Harbin Engineering University, majoring in structural impact dynamics.